AN AUTOMATED DEFECT CLASSIFICATION ALGORITHM FOR PRINTED DOCUMENTS

Onome Augustine Ugbeme[1], Eli Saber[1], Wencheng Wu[2]

1. **Dept. of Electrical Engineering, Rochester Institute of Technology, Rochester, NY 14623, USA.**
2. **Xerox Corporation, 800 Phillips Road, Webster, NY 14580, USA.**

{oau8082, esseee}@rit.edu, wwu@xeroxlabs.com

ABSTRACT

A method for automatically identifying image quality defects on printed documents is described. This method accepts a scanned image containing the defect and employs a three stage identification approach. The first stage involves performing a global thresholding procedure in order to expose the region(s) of interest and thus define a mask. In the second stage, a threshold value is chosen using some information of the histogram distribution. The derived object(s) is then made rotation and translation invariant via Principal Component Analysis normalization procedures. In the last stage, a classification is carried out on the pre-processed object(s). This approach has been tested on a database provided by Xerox Corporation yielding an 80.5% classification rate.

1. INTRODUCTION

Image quality stands among the most important outcomes of image acquisition and printing devices. In the past decade, we have seen a tremendous increase in the quality of printed documents due to significant technological advances in Non-Impact Printing. Present day print engines are required to produce consistent and stable image quality requirements as measured by various metrics and ultimately evaluated by customers. The current marketplace demands the best image quality from print engine suppliers at competitive costs with minimum downtime. Hence, the ability our vendors to achieve this reliably will ensure their company a leadership role in the printing industry.

However, even though the quality of printed documents has improved significantly over the past decade, the current print engines still possess a variety of image quality defects and artifacts (e.g. Deletion, Debris Centered Deletion (DCD), streaks, mottle, etc.) as shown in Figure 1 that often result from faults or degradations in the underlying imaging and electro photographic processes. These artifacts present themselves in a variety of shapes and sizes and could possibly occur in different locations on the print. Operator intervention is often required to perform corrective action to eliminate or reduce occurrences of defect(s). In some cases, new defects never encountered before are diagnosed and resolved as quickly as possible to minimize downtime. Therefore, the ability to successfully automate the defect detection process is vital to the minimization of downtime yielding higher profit margins. Attempts to achieve this goal were done by Iivarinen and Visa [1] in which they employ self-organizing maps (SOMs) to classify base paper defects.

In this paper, we propose a four stage algorithm to detect print engine deletion defects in an automated fashion. The defects classified include Deletion, Debris Centered Deletion (DCD), and a special case of DCD. Each of these defects tends to be distributed in an elliptical spatial arrangement. A Deletion is usually an elliptical region lighter than the background, while a DCD resembles a Deletion with the presence of a bead (or dark spot) approximately in the center of the deletion region. Additionally, a special case of DCD exists where the bead is missing due to accidental "rub off" by the electro photographic process. Appropriate image preprocessing and choice of image thresholds are determined automatically to ensure total automation of the procedure. The effectiveness of the proposed algorithm is demonstrated on an example database of defects provided by Xerox Corporation.

The remainder of this paper is organized as follows. In Section 2, the image pre-processing steps carried out in the underlying algorithm are discussed. Section 3 details the method employed for thresholding the scanned images. Section 4 discusses the normalization procedures. Section 5 outlines the feature extraction and classification procedure. Experimental results are presented in Section 6 and conclusions are drawn in Section 7.

2. PROPOSED ALGORITHM

The defect classification process is summarized in Figure 2. It is generally divided in four major steps, namely pre-processing, global thresholding, localized thresholding and classification. Each step is described in detail in subsequent

sections. The two stage thresholding process is undertaken in order to account for and remedy bead missing situations.

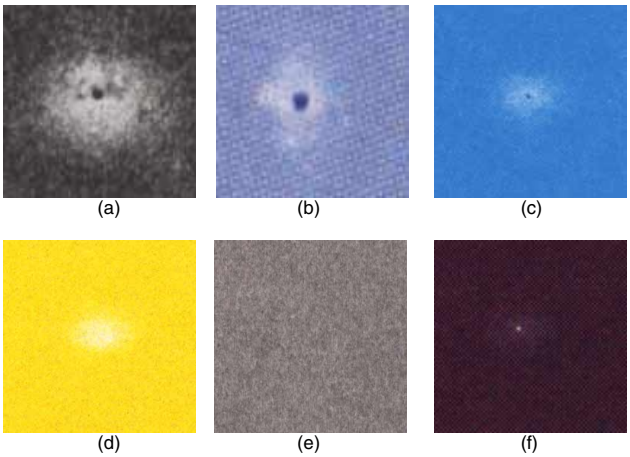

***Figure 1**: a-c) DCD defect samples, d) Deletion defect sample, e) Mottle defect sample, f) DCD with bead missing defect sample.*

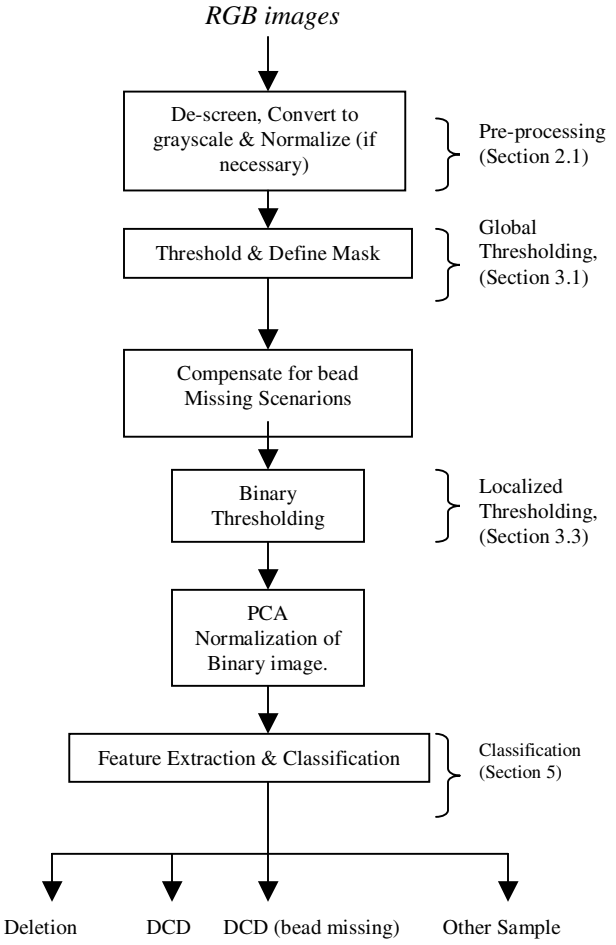

***Figure 2**: Flow-chart representing current algorithm.*

2.1. Image Pre-processing

Direct thresholding of scanned images, without prior image pre-processing, can lead to unpredictable results. Hence, it is essential to carry out some pre-processing steps prior to thresholding and subsequent classification. Since the input images are scanned, there is a tendency for the scanning process to pick up the halftone screen used to emulate the continuous tone during the substrate marking process [2]. This effect is undesirable and needs to be eliminated to guarantee reliable binarization results. We analyze the image power spectrum to determine the existence of high energy content that represents the signature of an underlying halftone screen. The screen is then reduced using a "notch" filtering operation yielding a continuous tone image that is appropriate for our proposed detection procedure. The above is shown in Figure 3.

***Figure 3**: Image de-screening process: a) Original screened image, b) De-screened image after removal of abnormal high energy at high frequencies.*

This process is independently applied on all three channels (R, G, and B) since the spectrum of each channel varies followed by a grayscale conversion. The grayscale conversion is achieved by formulating a maximum contrast image from all three channels:

$$f(x,y) = \min\{R(x,y), G(x,y), B(x,y)\} \tag{1}$$

Due to spatial variations during printing, a normalization procedure is carried out to prevent inaccurate results after thresholding as illustrated in Figure 4. This is necessary to ensure effective post-processing of the thresholded image in order to improve the classification accuracy. Figures 4c and 4b show the thresholding results with and without normalization on the image illustrated in Figure 4a. The local normalization (LN) process which efficiently eliminates the effect of uneven illuminations as described in [3]. The process is given by:

$$g(x,y) = \frac{f(x,y) - m_f(x,y)}{\sigma_f(x,y)} \tag{2}$$

where:

- $f(x,y)$ is the original image
- $m_f(x,y)$ is an estimation of a local mean of $f(x,y)$
- $\sigma_f(x,y)$ is an estimation of the local standard deviation
- $g(x,y)$ is the output image

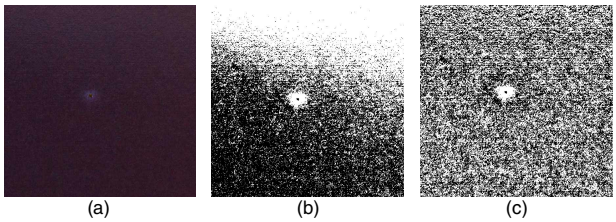

***Figure 4**: Importance of Local Normalization process: a) Input Image b) Thresholded image prior to using LN c) Thresholded image after using LN.*

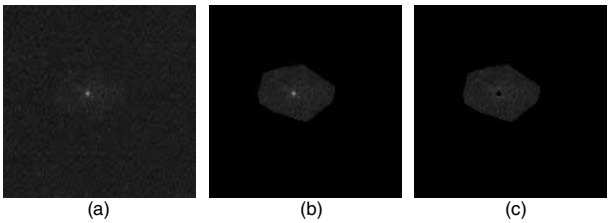

***Figure 5**: a) De-screened and grayscale equivalent of image in Figure 1h, b) Masked ROI, c) Bead added successfully.*

3. BINARY THRESHOLDING

3.1. Global Thresholding

Most thresholding mechanisms fail to successfully expose the Region of Interest (ROI) in the first stage. We have discovered that using a customized version of Niblack's thresholding criteria [4] produces the overall desired result. The threshold selection is chosen as

$$T_{global} = m_{global} + k \cdot \sigma_{global} \tag{3}$$

with k = *-0.1*. An example of the resultant binary image is depicted in Figure 4c.

An opening morphology operation (erosion followed by dilation) is carried out on the image. The structuring element was chosen as a disk having a radius of 3 pixels. A mask is then created over this region by utilizing its convex hull. The chosen procedure for bead missing recognition and possible replacement involves exhaustively thresholding the masked image until a small object greater than an empirically determined size is observed at an approximate centroid location. Figure 5 depicts the success of this process in effectively capturing and replacing the missing bead. The exposed ROI is then thresholded again using a process formulated by Ng [5] that modifies Otsu's [6] method.

3.2. Valley-Emphasis Thresholding criteria

Otsu's method [5] is one of the most referenced thresholding mechanisms and is primarily based on the clustering of gray-level data. Pixel values are assigned to one of two classes according to an optimal threshold candidate utilized to minimize the within-class variances. However, this process assumes a bimodal histogram of the image and gives satisfactory results when the number of pixels in each class are close to each other. From our observations, the distribution of pixels within the created mask tends to be almost unimodal hence Otsu's process yields inaccurate or noisy results.

It was observed that the best threshold for most of the images in the database is found somewhere at the base of the corresponding histograms. Hence, the probability of occurrence at the threshold value (p_t) should be small. According to Ng [5], an improved Otsu method was proposed which ensures that the chosen threshold value has a small probability of occurrence and, at the same time, preserves Otsu's idea by maximizing the between-class scatter. The valley-emphasis threshold is chosen as:

$$t_{opt} = Arg \underset{g\min \le t < g\max}{Max} \{(\omega_1(t)\mu_1(t)^2 + \omega_2(t)\mu_2(t)^2)(1-p_t)\} \tag{4}$$

where ω_i and μ_i respectively represent the probability and mean of class i = *1,2*.

The weight (1-p_t) guarantees that the chosen threshold will have a small probability since a smaller p_t value gives a larger weight. The optimal threshold thus resides at the bottom rim of the histogram. Once the masked region has been successfully thresholded, the binary image is passed to the next stage of orientation and location normalization via principal component analysis (PCA) routines.

4. NORMALIZATIONS

Since the database consists of defects at multiple scales, orientations and variations, normalization processes need to be carried out to attain an appreciable level of uniformity among the binarized version of the images. In [7], before projections of logos are obtained, the logo images are first normalized by performing PCA directly on the set of pixels representing the logo. The same process is undertaken here. The covariance matrix of the deletion area is computed followed by the derivation of its eigenvalues and eigenvectors. The binary image is then rotated so as to align the principal component direction with the horizontal. Location/Translation normalization is achieved by moving the centroid of the rotated image to the center of the image. Features are then extracted from within an elliptical region of the normalized binary image.

5. FEATURE EXTRACTION AND CLASSIFICATION

Since the defects tend to be distributed in an elliptical arrangement, the contour of the binary image is directly compared to a contour of an elliptical fit using Hausdorff Distance (HD). This ensures the elimination of regions dissimilar to a regular defect. An elliptical region is obtained by using the spatial coordinates of the ROI to form a covariance matrix. We utilize the same process carried out by Saber [8] in which eigenvalues and eigenvectors of the covariance matrix are used as parameters for the elliptical equation. Images with HDs above an empirically determined threshold are rejected or classified as unknown images for future processing.

The largest and most proximal hole to the centroid of the ellipse is captured and classification is carried out using the area as the principle feature. The classification is performed using an empirically derived threshold to decide which class the defect belongs to. Furthermore, a measure of the classification confidence is given by its Mahalanobis distance from the center of the ellipse.

6. EXPERIMENTAL RESULTS

Preliminary tests were carried out on 200 images provided by Xerox Corporation. Of the 200 images (see Table 1), 89 were DCDs, 76 were deletions, 12 were Mottle images and 23 were other images comprising of streaks, logos etc. Of the 89 DCD images, 8 had missing beads and can easily be classified as deletions instead of DCDs by a human observer. All the images are of RGB type with varying resolutions and dimensions.

The performance of our proposed algorithm is documented in Table 1. The algorithm was applied to all images without any manual intervention. Thresholds were computed directly and automatically from the images during the classification process.

From the table, it can be easily seen that 69 out of 89 DCDs were correctly classified yielding a 77.5% accuracy. The remaining 20 were mis-classified as deletions due to the low contrast in the image where the bead was not visible. Given the lack of contrast and the absence of the bead in the above mentioned images, it is entirely possible that the originals were mis-labeled by the operator during the acquisition process.

The results for the remaining categories is shown in Table 1, where the mottle and deletion images were classified with a 100% and 90.8% accuracy respectively. The total correct classification rate weighted by the number of images is 80.5%.

True Class	Number of images	CLASSIFICATION RESULTS			
		DCD	Deletion	Unknown	Accuracy
DCD	89	69	20		77.5%
Deletion	76	7	69		90.8%
Mottle	12			12	100%
Other	23	4	1	18	78.3%

***Table 1**: Confusion matrices*

7. CONCLUSION AND FUTURE WORK

In this paper, an algorithm for automatically identifying and classifying defects in printed documents is proposed. Due to large variations between elements of the same class, several pre-processing techniques were carried out on each image to attain some level of uniformity amongst the samples. Furthermore, thresholding is carried out in two stages to accurately separate objects of interest from their background. The results indicate a 80.5% accuracy in classification. Future research will involve modeling the images as modified Gaussian surfaces from which features can be computed based on the corresponding Gaussian parameters.

ACKNOWLEDGEMENTS

This research was funded in part by Center for Electronics and Imaging Systems (CEIS), a NYSTAR-designated Center for Advanced Technology, Xerox Corporation, and the Electrical Engineering Department at the Rochester Institute of Technology.

REFERENCES

[1] J. Iivarinen and A. Visa, "An Adaptive Texture and Shape Based Defect Classification," Proceedings of the 14th International Conference on Pattern Recognition, Vol. 1, pp. 117-122, Brisbane, Australia, Aug. 1998.

[2] G. Sharma, et al., "Methods and apparatus for identifying marking process and modifying image data based on image spatial characteristics." US Patent #6353675B1, Mar. 2002.

[3] X. Xie and K. Lam, "An Efficient Method for Face Recognition under Varying Illumination," 2004.

[4] W. Niblack, "An Introduction to Image Processing", pp. 115 – 116, Prentice-Hall, Englewood Cliffs, NJ (1986).

[5] H. Ng, "Automatic thresholding for Defect Detection," Proceedings of the 3rd International Conference on Image and Graphics, 2004.

[6] N. Otsu, "A threshold selection method from gray-level histogram," IEEE Transactions on Systems, Man and Cybernetics, SMC-8, pp. 62-66, 1978.

[7] M. Y. Jaisimha, "Wavelet Features for Similarity based Retrieval of Logo Images," SPIE Vol. 2660, 1996.

[8] E. Saber and A. Murat Tekalp, "Frontal-view face detection and facial feature extraction using color, shape and symmetry based cost functions," Pattern Recognition Letters 19, pp. 669-680, 1998.

Biography

Onome Augustine Ugbeme is currently pursuing his M.S. degree in Electrical Engineering at the Rochester Institute of Technology, Rochester, NY. He obtained a B.S. degree in Electrical Engineering from the University of New Orleans, New Orleans, LA in 2004. He is a member of the IEEE, the National Society of Black Engineers, the Tau Beta Pi and Eta Kappa Nu Honor Societies. At the Rochester Institute of Technology, he is a teaching and a research assistant working on identifying defects in images.